Enhanced Direct Torque Control Using a Three-Level Voltage Source Inverter

R. Zaimeddine[1], E.M. Berkouk[2]

Abstract –The objective of this paper is to study a new control structure for the sensorless induction machine dedicated to electrical drives by using a three-level voltage source inverter (VSI). The output voltages of the three-level VSI can be represented by four groups: the zero voltage vectors, the small voltage vectors, the middle voltage vectors and the large voltage vectors in (d , q) plane. The amplitude and the rotating velocity of the flux vector could be freely controlled while both the fast torque and the optimal switching logic are obtained. The selection is based on the value of the stator flux and the torque. Both approaches are simulated for an induction motor. The results obtained have shown a superior performance over the conventional DTC one without the need of the mechanical sensor.

Keywords - Direct torque control, field oriented control, induction motor, sensorless vector control, flux estimators, switching strategy optimisation, multi-level inverter, neural-point clamped.

I. Introduction

Vast development in capacity and switching frequency of the power semiconductor devices, together with the continuous advancement of the power electronics technology have caused many changes in the static power converter systems and industrial motor drive areas. The conventional GTO inverters have limitation in their dc-link voltage. Hence the series connections of the existing GTO thyristors have been essential in realizing high voltage and large capacity inverter configurations with the dc-link voltage [1]. The vector control of the induction motor drive has made it possible for applications that require fast torque control such as traction [2]. In a perfect field oriented control, the decoupling characteristics of the flux and torque are affected significantly by the parameter variation of the machine.

This paper studies the control scheme for the direct torque and flux control of the induction machines which are fed by a three-level inverter by using a switching table. In this method, the output voltage is selected and applied sequentially to the machine through a look–up table so that the flux is kept constant and the torque is controlled by the rotating speed of the stator flux. The direct torque control (DTC) is one of the actively researched control schemes which is based on the decoupled control of flux and torque. It provides a very quick and robust response with simple control [3],[4].

Digital ref: A070101123

[1]Department of Electrical Engineering,'Signals and Systems' Research laboratory, University of M'hamed Bougara, Boumerdes
e-mail : rabah_zaimeddine@yahoo.fr
[2] Process Control Laboratory, National Polytechnic School, Algiers, Algeria

The paper first received on 8 Mar 2005 and in revised form 1 Feb 2006.

The performances permit such a system to be applicable in areas such as railway traction, ac drives.

II. Three-Level Inverter Topology and the NPC Voltage Source

Fig. 1 shows the schematic diagram of the neutral point clamped (NPC) three-level VSI. Each phase of this inverter consists of two clamping diodes, four GTO thyristors and four freewheeling diodes.

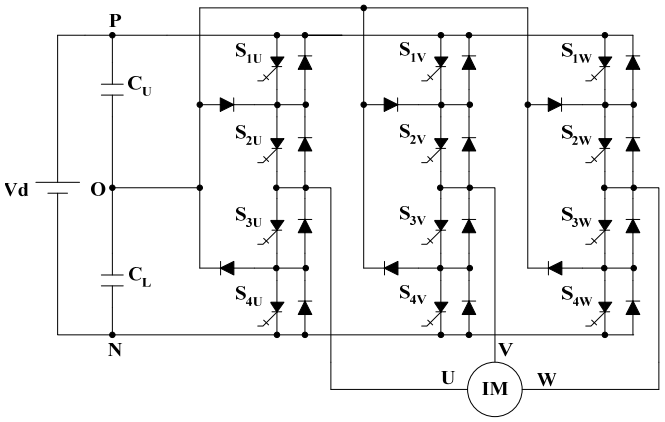

Fig. 1: Schematic diagram of a three-level GTO inverter

Table 1 shows the switching states of this inverter. Since three kinds of switching states are existed in each phase, a three level inverter has 27 switching states.

Table 1: Switching states of a three-level inverter

Switching states	S_1	S_2	S_3	S_4	V_N
P	ON	ON	OFF	OFF	V_d
O	OFF	ON	ON	OFF	$V_d/2$
N	OFF	OFF	ON	ON	0

A two-level inverter is only capable in producing six non-zero voltage vectors and two zero vectors [2]. Fig.2 shows the representation of the space voltage vectors of a three-level inverter for all switching states.

According to the magnitude of the voltage vectors, we divide them into four groups : the zero voltage vectors (V_0), the small voltage vectors (V_1 , V_4 , V_7 , V_{10} , V_{13} , V_{16}), the middle voltage vectors (V_3 , V_6 , V_9 , V_{12} , V_{15} , V_{18}), the large voltage vectors (V_2 , V_5 , V_8 , V_{11} , V_{14} , V_{17}).

The zero voltage vector (ZVV) has three switching states, the small voltage vector (SVV) has two, and both the middle voltage vector (MVV) and the large voltage vector (LVV) have only one [1].

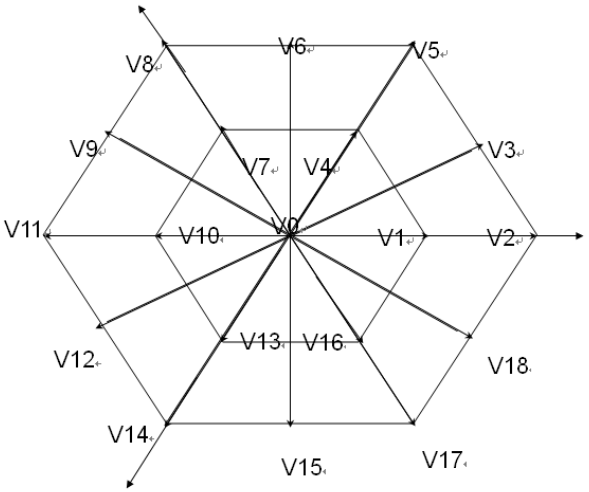

Fig. 2: Space voltage vectors of a three-level inverter

III. Induction Machine

Torque control of an asynchronous motor can be achieved on the basis of its model developed in a two axes (d , q) reference frame stationary with the stator winding. In this reference frame and with the conventional notations (appendix), the electrical mode is described by the following equations:

$$\frac{di_{sd}}{dt}=\frac{1}{\sigma T_r L_s}\varphi_{sd}+\frac{p\Omega}{\sigma L_s}\varphi_{sq}-\frac{1}{\sigma}\left(\frac{1}{T_r}+\frac{1}{T_s}\right)i_{sd}-p\Omega i_{sq}+\frac{1}{\sigma L_s}V_{sd} \quad (1)$$

$$\frac{di_{sq}}{dt}=-\frac{p\Omega}{\sigma L_s}\varphi_{sd}+\frac{1}{\sigma T_r L_s}\varphi_{sq}-\frac{1}{\sigma}\left(\frac{1}{T_r}+\frac{1}{T_s}\right)i_{sq}+p\Omega i_{sd}+\frac{1}{\sigma L_s}V_{sq} \quad (2)$$

$$\frac{d\varphi_{sd}}{dt}=V_{sd}-R_s i_{sd} \quad (3)$$

$$\frac{d\varphi_{sq}}{dt}=V_{sq}-R_s i_{sq} \quad (4)$$

$$\varphi_{sd}=L_s\, i_{sd}+L_m\, i_{rd} \quad (5)$$

$$\varphi_s q=L_s\, i_{sq}+L_m\, i_{rq} \quad (6)$$

$$\varphi_{rd}=L_r\, i_{rd}+L_m\, i_{sd} \quad (7)$$

$$\varphi_{rq}=L_r\, i_{rq}+L_m\, i_{sq} \quad (8)$$

The mechanical mode associated to the rotor motion is described by:

$$J\frac{d\Omega}{dt}=\Gamma_{em}-\Gamma_r(\Omega) \quad (9)$$

$\Gamma_r(\Omega)$ and Γ_{em} are respectively the load torque and the electromagnetic torque developed by the machine.

IV. Stator Flux and Torque Estimation

Basically, DTC schemes require the estimation of the stator flux and torque. The stator flux evaluation can be carried out by different techniques depending on whether the rotor angular speed or (position) is measured or not. For sensorless application, the "voltage model" is usually employed. The stator flux can be evaluated by integrating from the stator voltage equation.

$$\varphi_S(t)=\int(Vs-R_S I_S)dt \quad (10)$$

This method is very simple requiring only the knowledge of the stator resistance. The effect of an error in Rs is usually negligible at high excitation frequency but it becomes more serious as the frequency approaches zero [5].

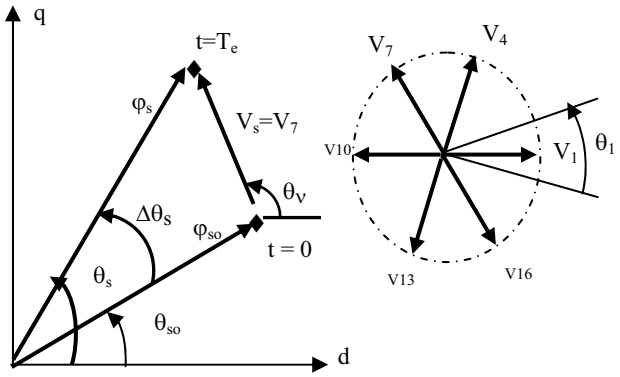

Fig. 3: Flux deviation

Fig.3 shows the representation of the space voltage vectors for one group of the switching states. The deviation that is obtained at the end of the switching period Te can be approached by the first order Taylor Seri as below.

$$\Delta\varphi_s \approx V_s.T_e.\cos(\theta_v-\theta_s)$$
$$\Delta\theta_s \approx T_e.\frac{V_s.\sin(\theta_v-\theta_s)}{\varphi_{so}} \quad (11)$$

Considering the combination of states of switching functions Su, Sv, Sw. Fig.3 shows the adequate voltage vector selection in which we can increase or decrease the stator flux amplitude and phase in order to obtain the required performances. The electric torque is estimated from the flux and current information as [2]:

$$\Gamma_{em}=p\,(i_{sq}\varphi_{sd}-i_{sd}\varphi_{sq}) \quad (12)$$

V. Principle of Direct Torque Control

Fig. 4 shows a block diagram of the DTC scheme. The reference values of flux, φs^*, and torque, Γ_{em}^*, are compared to their actual values and the resultant errors are fed into a two level comparator of flux and torque, [2].
The stator flux angle, θ_s is calculated by:

$$\theta_S=\arctan\frac{\varphi_{sq}}{\varphi_{sd}} \quad (13)$$

This is also quantified into 6 levels depending on which sector the flux vector falls into. Different switching strategies can be employed to control the torque depending on whether the flux has to be reduced or increased. Each strategy affects the drive behavior in terms of torque and current ripple, switching frequency and two or four-

quadrant operation capability. Assuming the voltage drop R_s i_s small, the head of the stator flux φ_S moves in the direction of stator voltage V_s at a speed proportional to the magnitude of V_s according to

$$\Delta\varphi_S = V_s\, T_e \qquad (14)$$

The switching configuration is made step by step, in order to maintain the stator flux and torque within limits of the two hysteresis bands. Where T_e is the period that the voltage vector is applied to the stator winding, appropriate selection of the voltage vector step by step, makes it possible to drive φ_s along a prefixed track curve.

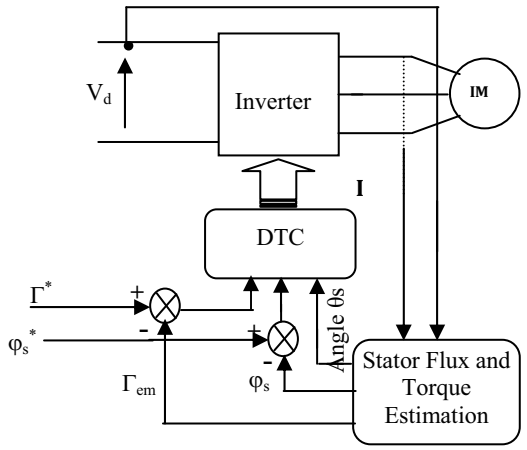

Fig. 4: Block diagram of direct torque control

Assuming the stator flux vector lying in the k-th sector (k=1,2,3,4,5,6) of the (d , q) plane, in the case of three level inverter, to improve the dynamic performance of DTC at low speed and to allow four-quadrant operation, it is necessary to involve the voltage vectors V_{K-1} and V_{K-2} in torque and flux control. In the following, V_{K-1} and V_{K-2} will be denoted "backward" voltage vectors in contraposition to "forward" voltage vectors utilised to denote V_{K+1} and V_{K+2}. A simple strategy which makes use of these voltage vectors is shown in table2. The conventional DTC for an induction motor fed by thee-level voltage source inverter has been studied, [6].

Table 2: Selection strategy for four-quadrant operation

		$\Gamma_{em}\uparrow$	$\Gamma_{em}\downarrow$
φ_s	$\uparrow$	V_{K+1}	V_{K-1}
φ_s	$\downarrow$	V_{K+2}	V_{K-2}

For steady operating conditions, equations (12) that describe the machine torque can be transformed to a sinus function:

$$\Gamma_{elmo} = \Gamma_{\max o}.\sin 2\gamma_o \qquad (15)$$

$\Gamma_{\max o}$ *and* γ_o are equation respectively torque and the difference angle between stator and rotor flux vectors.

$$\Gamma_{\max o} = p.\frac{1-\sigma}{2.\sigma.L_s}.\varphi_{so}^2 \quad ; \quad \gamma_o = \theta_{so} - \theta_{ro} \qquad (16)$$

Equations (15) and (16) are established with the assumption that stator flux and rotor closed values are in steady state. For the disturbed states, the stator flux angle θ_s has in practice a fast dynamic mode as compared to the rotor flux angle θ_r. If these two assumptions are held the effect of stator vector voltage on the machine torque can be expressed by the first order Taylor expansion as shown below:

$$\Delta\Gamma_{elm} \approx K_\varphi.\Delta\varphi_s + K_\theta.\Delta\theta_s \qquad (17)$$

The sensitivity coefficients Kφ and Kθ are defined by:

$$\begin{cases} K_\varphi = \dfrac{d\Gamma_{elm}}{d\varphi_s} = \dfrac{2}{\varphi_{so}}.\Gamma_{elmo} \\ K_\theta = \dfrac{d\Gamma_{elm}}{d\theta_s} = 2.\Gamma_{\max o}.\cos 2\gamma_o \end{cases} \qquad (18)$$

Linking equations (11), (17) and (18) leads to:

$$\Delta\Gamma_{elm} = 2.\frac{V_s.T_e}{\varphi_{so}}.\Gamma_{elmo}.\cos(\theta_v - \theta_{so}) + \frac{2.V_s.T_e}{\varphi_{so}}.\sqrt{\Gamma_{\max o}^2 - \Gamma_{elmo}^2}.\sin(\theta_v - \theta_{so}) \qquad (19)$$

This shows the feasibility torque control by a well selected vectors voltage $\overline{Vs}$ [6].

According to the strategy, the stator flux vector is required to rotate in both positive and negative directions. Even at a very low shaft speed, large negative values of rotor angular frequency can be achieved, which are required when the torque is to be decreased very quickly. Furthermore, the selection strategy represented in table 2 allows good flux control to be obtained even in the low speed range. However the high dynamic performance which can be obtained by utilising voltage vectors and having large components tangential to the stator vector locus, have implied a very high switching frequency.

VI. Switching Strategy for Conventional Direct Torque Control

The switching strategy in the order of the sector θs, is illustrated by each table.

θ1

E_Γ \ E_φ	P	Z	N
PL	5	4	8
PS	3	4	6
ZE	0	0	0
NS	18	0	12
NL	17	13	14

θ2

E_Γ \ E_φ	P	Z	N
PL	8	7	11
PS	6	7	12
ZE	0	0	0
NS	3	0	15
NL	2	16	17

θ3

E_Γ \ E_φ	P	Z	N
PL	11	10	14
PS	9	10	15
ZE	0	0	0
NS	6	0	18
NL	5	1	2

θ4

E_Γ \ E_φ	P	Z	N
PL	14	13	17
PS	12	13	18
ZE	0	0	0
NS	9	0	3
NL	8	4	5

θ5

E_Γ \ E_φ	P	Z	N
PL	17	16	2
PS	15	16	3
ZE	0	0	0
NS	12	0	6
NL	11	7	8

θ6

E_Γ \ E_φ	P	Z	N
PL	2	1	5
PS	18	1	6
ZE	0	0	0
NS	15	0	9
NL	14	10	11

VII. An Enhanced Direct Torque Control

A switching table is used to select the best output voltage depending on the position of the stator flux and the desired action on the torque and stator flux. The flux position in the (d , q) plane is quantified in twelve sectors. Alternative tables are also existed for the specific operation mode. In the case of a two-level inverter, it is possible to expand the optimal vector selection in order to include a larger number of voltage vectors produced by a three-level inverter. The appropriate vector voltage is selected in such order that reduces the number of commutation and the level of steady-state ripple.

For the flux control, let the variable E_φ ($E_\varphi=\varphi_s^*-\varphi_s$) be located in one of the three regions fixed by the contraints:

$$E_\varphi < E_{\varphi\,min}\ ,\ E_{\varphi\,min} \le E_\varphi \le E_{\varphi\,max}\ ,\ E_\varphi > E_{\varphi\,max}\ .$$

The switable flux level is then bounded by $E_{\varphi\,min}$ and $E_{\varphi max}$. The flux control is made by the two-level hysteresis comparator. Three regions for the flux location are noted, flux as in fuzzy control schemes, by $E_{\varphi n}$ (negative), $E_{\varphi z}$ (zero) and $E_{\varphi p}$ (positive).

A high level performance torque control is required. To improve the torque control let of the mismacth E_Γ ($E_\Gamma = \Gamma_{em}^* - \Gamma_e$) to belong to one of the five regions defined by the contraints :

$$E_\Gamma < E_{\Gamma min2}\ ,\ E_{\Gamma min2} \le E_\Gamma \le E_{\Gamma min1}\ ,\ E_{\Gamma min1} \le E_\Gamma \le E_{\Gamma max1}\ ,$$
$$E_{\Gamma max1} \le E_\Gamma \le E_{\Gamma max2} \text{ and } E_{\Gamma max2} < E_\Gamma\ .$$

The five regions defined for torque location are also noted , as in fuzzy control schemes, by $E_{\Gamma nl}$ (negative large), $E_{\Gamma ns}$ (negative small), $E_{\Gamma z}$ (zero), $E_{\Gamma ps}$ (positve small), $E_{\Gamma pl}$ (positve large). The torque is then controlled by an hysteresis comparator built with two lower bounds and two upper known bounds [7].

VIII. Switching Strategy for an Enhanced Direct Torque Control

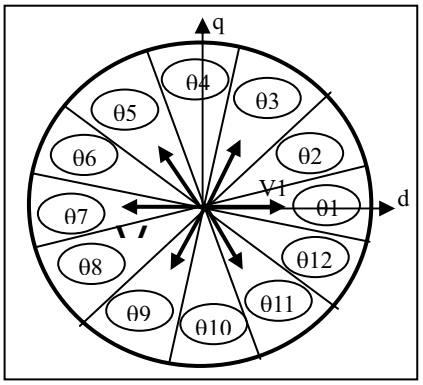

Fig. 5: Location sectors of flux approach

The switching strategy in the order of the sector θs, is illustrated by each tables. The flux and torque control by vector voltage has a desecrate behavior in nature.

The vector voltage selection can then be made with an established table of knowledge and rules that have three inputs: flux mismatch E_φ, the torque mismatch and the rank k of the location sectors of θ_s shown by the fig. 5. It is also based on the vector diagram shown in fig.3.
Looking at the position of the flux in the sector θ_1, for a small decrease in flux and torque, state 15 is selected. For a small increase in flux in torque, state 3 is selected. For a small decrease in flux and large decrease in torque, state 14 is selected. For a small decrease in torque and a constant flux, state 0 is selected. Thus the selection changes as the position of the flux vector changes.

In fact it simply verifies that the same vector could be adequate for a set of value of θ_s. The number of sectors should be set as large as possible in order to have an adequate decision. For this reason, we propose a new approach for direct torque control by using a three-level inverter based on twelve regular sectors noted by θ_1 to θ_{12}.

θ1

E_Γ \ E_φ	P	Z	N
PL	5	4	8
PS	3	4	9
ZE	0	0	0
NS	18	0	15
NL	17	13	14

θ2

E_Γ \ E_φ	P	Z	N
PL	5	4	8
PS	6	7	9
ZE	0	0	0
NS	18	0	15
NL	2	16	17

θ3

E_Γ \ E_φ	P	Z	N
PL	8	7	11
PS	6	7	9
ZE	0	0	0
NS	3	0	18
NL	2	16	17

θ4

E_Γ \ E_φ	P	Z	N
PL	8	7	11
PS	9	10	12
ZE	0	0	0
NS	3	0	18
NL	15	1	2

θ5

E_Γ \ E_φ	P	Z	N
PL	11	10	14
PS	9	10	12
ZE	0	0	0
NS	6	0	3
NL	5	1	2

θ6

E_Γ \ E_φ	P	Z	N
PL	11	10	14
PS	12	13	15
ZE	0	0	0
NS	6	0	3
NL	8	4	5

θ7

E_Γ \ E_φ	P	Z	N
PL	14	13	17
PS	12	13	15
ZE	0	0	0
NS	9	0	6
NL	8	4	5

θ8

E_Γ \ E_φ	P	Z	N
PL	14	13	17
PS	15	16	18
ZE	0	0	0
NS	9	0	6
NL	11	7	8

θ9

E_Γ \ E_φ	P	Z	N
PL	17	16	2
PS	15	16	18
ZE	0	0	0
NS	12	0	9
NL	11	7	8

θ10

E_Γ \ E_φ	P	Z	N
PL	17	16	2
PS	18	1	3
ZE	0	0	0
NS	12	0	9
NL	14	10	11

θ11

E_Γ \ E_φ	P	Z	N
PL	2	1	5
PS	18	1	3
ZE	0	0	0
NS	15	0	12
NL	14	10	11

θ12

E_Γ \ E_φ	P	Z	N
PL	2	1	5
PS	3	4	6
ZE	0	0	0
NS	15	0	12
NL	17	13	14

IX. The Simulation Results

The validity of the proposed DTC algorithm for the three-level voltage source inverter is proved by the simulation results using Matlab-Simulink. The parameters of the motor are given in the Appendix. The used flux and torque mismathes for the approach are expressed in percentage with respect to the flux and torque reference values.

$$E_{\varphi\,max} = 3\% \text{ , } E_{\varphi\,min} = -3\% \text{ , } E_{\Gamma min1} = -0.8\% \text{ ,}$$
$$E_{\Gamma min2} = -3\% \text{ , } E_{\Gamma max1} = 0.8\% \text{ , } E_{\Gamma max2} = 3\%.$$

The simulation results illustrate both the steady state and the transient performance of the proposed torque control scheme. However, the machine has been supposed to run at load.

$$\Gamma_r = \left(\frac{\Gamma_{em}}{\Omega_{ref}} - K_f \right).\Omega \qquad (20)$$

The FFT of the current waveform of phase (a) is shown in Fig. 6. The phase currents generated by the three-level inverter have low harmonic contents with the new approach (5.95 % THD).

Fig.7 shows the phase current and flux for the steady state operation and the transient régime at 9 N.m with 0.9 Wb. The wave form of the stator current is closed to a sinusoidal signal. The trajectory of the flux in the case of the new approach is nearly a circle and it answers more quickly, (9ms), compared to the flux response in the conventional DTC.

Fig.8 shows the torque reverse response from + 9 N.m to - 9 N.m and flux for 0.9 Wb. The output torque reaches the new reference torque in about 2 ms, fast torque response is obtained.

Low torque ripple is observed in Fig.9. One nearly has the same rate of harmonic for the two approaches.

Fig.10 shows an overtaking of the current which is acceptable. The simple voltage response of the motor commutes to a variable frequency in the two approaches.

Fig.11 shows the torque response for a linear change in the torque reference, a good follow-up of the trajectory is obtained with a control of the stator flux that is achieved. The stator current wave form is shown more closely to the suitable sinusoidal signal. From this analysis, high dynamic performance, good stability and precision have been achieved.

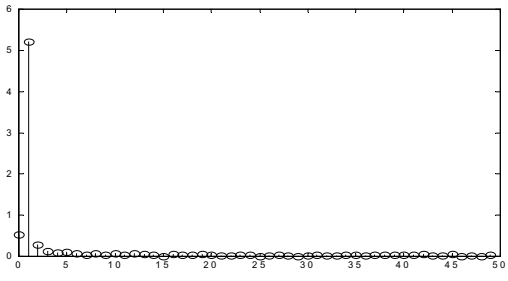

Fig. 6: Current harmonics enhanced

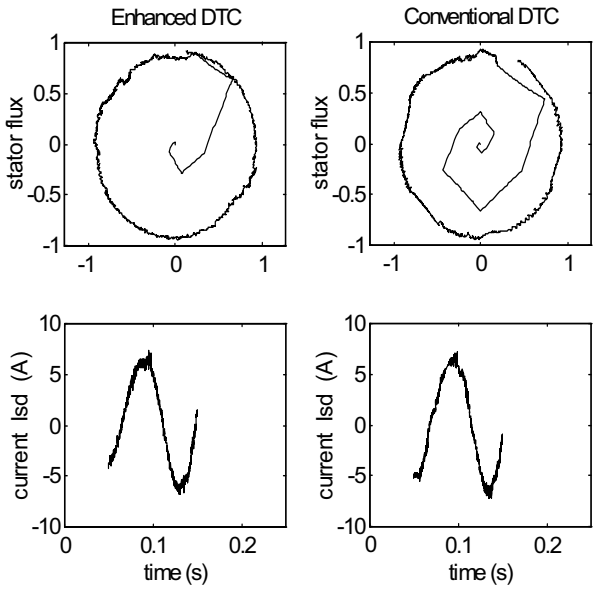

Fig. 7: Vector flux locus and current response

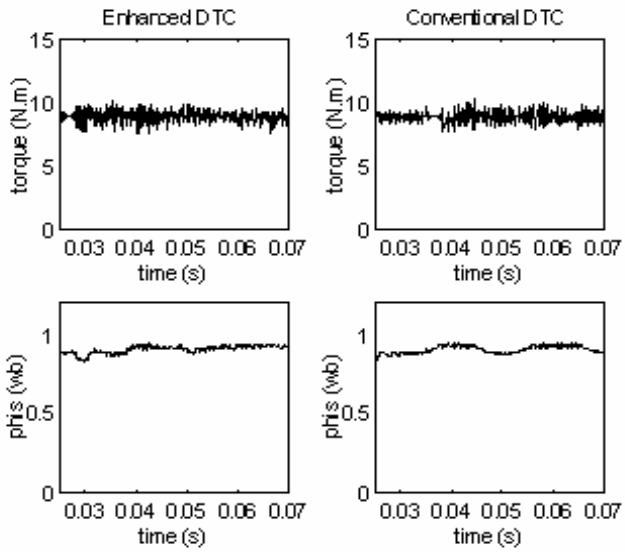

Fig. 8: Torque and flux response

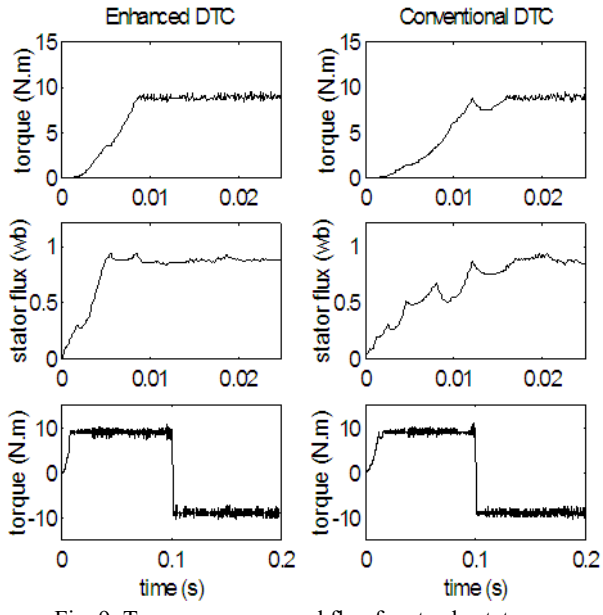

Fig. 9: Torque response and flux for steady state

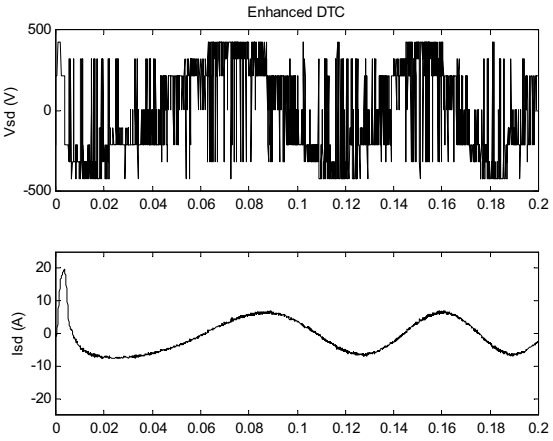

Fig. 10: The simple voltage and current response

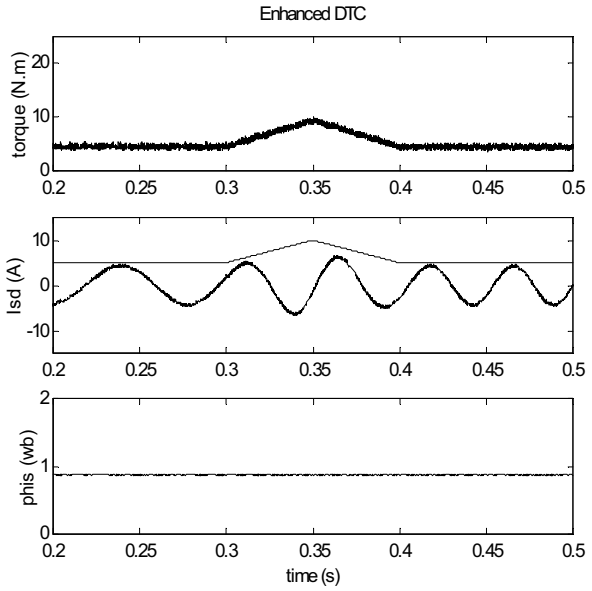

Fig. 11: Torque, stator flux and current response

X. Conclusion

The direct torque control DTC was introduced to provide a fast and well dynamic torque which is considered as an alternative to the field oriented control FOC technique. Two problems usually associated with the DTC drives which are based on hysteresis comparators, are the variable switching frequency and the inaccurate stator flux estimation. These have found to have a degrading effect in the drive performance. Another issue is concerned with the stability problem of the input DC voltage of the inverter, in which it is under survey.

The effect of the proposed method has been proven by the simulations conducted. It is concluded that the proposed control produces better results for transient state operation than that of the conventional control.

In this paper, a DTC systems using three-level GTO voltage source inverter is presented. It is found suitable for the high-power and high-voltage applications. Enhancement has been made on the DTC approach by introducing the two multi-level hysteresis comparators for flux and torque control. It imposes the flux angle detection procedure by defining twelve sectors of space and establishes a larger table of knowledge rules.
From the analysis of these results establish the following remarks:

The enhanced approach has a fast torque and flux response as compared to the conventional DTC. The amplitude of the torque ripples in steady state is closed for the two approaches.

List of The Used Notations

s , r : indices variables; L : magnetizing Inductance; L_m : mutual inductance ; V : voltage ; i : current ; φ : flux ; R : resistance ; Γ_{em} : electromagnetic torque ; J : rotor inertia ; P : number of pairs of poles ; ω_s : statoric pulsation ; V_d : dc-link voltage ; K_f : friction Coefficient ; Te : sampling time ; E : error of the variables; T_r : rotor time response ; T_s : stator time response.

ω_r : electric rotor speed ; $\Omega = p\,\omega_r$.

σ : Leakage coefficient, $\sigma = 1 - \frac{L_m^2}{Ls.Lr}$

INDUCTION MOTOR PARAMETERS
Rated power : 1.5 kW ; Rated voltage : 220 V ; Rated speed : 1420 rpm ; Rated frequency : 50 Hz ; Rotor resistance : 3.805 Ω ; Stator inductance : 0.274 H ; Rated current : 3.64 A (Y) et 6.31 (Δ) ; Stator resistance : 4.85 Ω ; Rotor inductance : 0.274 H ; Magnetizing Inductance : 0.258 H ; Number of poles : 2 ; Rotor inertia : 0.031 kg.m^2 ; Friction Coefficient : 0.008 N.m.s/rd ; Vd = 514 V ; Te =100 μs.

References

[1] Y.H. Lee, B.S. Suh and D.S. Hyan, "A Novel PWM Scheme for a Three-Level Voltage Source Inverter with GTO Thyristors", IEEE Trans. on Ind. Appl, Vol. 33, No. 2, March-April 1996, pp. 260-268.

[2] I. Takahashi and T. Noguchi, "A New Quick-Response and High-Efficiency Control Strategy of an Induction Motor", IEEE Trans. On IA, Vol. 22, No. 5, September-October 1996, pp. 820-827.

[3] J.C. Trounce, S.D. Round and R.M. Duke, "Comparison by Simulation of Three-Level Induction Motor Torque Control Schemes for Electrical Vehicle Applications", Proc. Of International Power Engineering Conference, Vol. 1, May 2001, pp. 294-299.

[4] Xuezh. Wu and L. Huang, "Direct Torque Control of Three-Level Inverter Using Neural Networks as Switching Vector Selector", IEEE-IAS, Annual Meeting, 30 September- 04 October 2001.

[5] D. Casadei, G. Grandi, G. Serra and A. Tani, "Switching Strategies in Direct Torque Control of Induction Machines", ICEM 94, Vol. 2, 1994, pp. 204-209.

[6] R. Zaimeddine and E.M. Berkouk, " ANovel DTC Scheme for a Three-Level Voltage Source Inverter with GTO Thyristors", SPEEDAM 2004, Symposium on Power Electronics, Electrical Drive, Automation & Motion, June, Vol. 2, 16th-18th June 2004, pp. F1A-9-F1A-12.

[7] F. Bacha, A. Sbai and R. Dhifaui, "Tow Approaches for Direct Torque Control of an Induction Motor", CESA Symposium on Control, Vol. 1, March 1998, pp. 562-568.